Image Cover Sheet

CLASSIFICATION	SYSTEM NUMBER 507459
UNCLASSIFIED	

TITLE

ASSESSING THE LONG TERM DURABILITY OF GLASS FIBRE COMPOSITES

System Number:

Patron Number:

Requester:

Notes:

DSIS Use only:

Deliver to:

ASSESSING THE LONG TERM DURABILITY OF GLASS FIBRE COMPOSITES

Alan J. Russell

Esquimalt Defence Research Detachment
CFB Esquimalt, Bldg. 199
PO BOX 17000 STN FORCES
VICTORIA, BC V9A 7N2
Canada

ABSTRACT

This paper describes part of a test program being carried out to substantiate the long term durability of glass fibre re-inforced composites for use in sonar domes and other Naval applications. This program, which was designed to encompass the combined effects of fatigue loading, impact damage and the marine environment, is generating data for material selection purposes as well as providing insight into degradation mechanisms. The testing reported here includes cyclic loading of 9 mm thick woven fabric composite laminates loaded in four point bending at R-ratios of R = 0.1 and R = -1 (fully reversed) as well as under bi-axial conditions (also at R= 0.1). An approach for predicting impact resistance is described and some results are presented which show the level of protection afforded by several different elastomeric coatings to 10 mm thick panels subjected to low velocity impact. In addition, the nature of the micro-cracking observed in two different glass fibre materials subjected to the aforementioned tests is compared.

INTRODUCTION

Although the long term durability of composite materials in marine environments has been well established and in spite of their generally superior resistance to corrosion and fatigue (compared to metals) designers are often faced with having to demonstrate that a particular material will survive in a given application. Degradation over time can be caused by a number of factors including fatigue loading, accumulation of impact damage and exposure to various environmental agents including moisture, excessive temperatures (both high and low) and ultraviolet radiation. In most marine applications, detailed information pertaining to these aspects of the operating environment may be unavailable while for many material systems relevant substantiating test data may be incomplete or may be too expensive and/or too time consuming to generate. In these circumstances, designers are often forced to reduce stress levels using well accepted but conservative rule-of-thumb criteria [1]. The lack of extensive test data also

makes it difficult to assess the long term durability implications of design and process modifications.

In the case of glass fibre re-inforced plastics the degradation process often includes a stage where "stress whitening" is evident. Certainly, both fatigue loading and sub-critical impacts can produce a whitening associated with the formation of micro-cracks in the matrix and at the fibre/matrix interface. These cracks can then short circuit the normally slow diffusion of moisture into the laminate. It is therefore reasonable to expect some level of synergism amongst the different factors controlling long term durability and new approaches are being taken to better demonstrate some of these effects [2]. In this paper some of the methodology that is being used to investigate and substantiate the long term durability of glass fibre re-inforced materials being considered for use in sonar domes and other Naval applications is described. This work includes investigating fatigue behaviour under realistic loading conditions and generating low velocity impact data suitable for input into a dynamic structural response model. As well as providing design data, the test program was also intended to clarify the mechanisms of damage growth and the role that seawater and other environmental effects play in the degradation process. Both optical and electron microscopy are being used to characterize and monitor damage growth.

FATIGUE TESTING

For most glass fibre composites, fatigue is a process that begins with micro-cracking or local deformation of the matrix, will likely involve interfacial shear failures between fibres and matrix and will eventually lead to fibre breakage and final failure [3]. While many of the material parameters that influence fatigue life have long been identified, eg. the strain to failure of the matrix, the fibre volume fraction and the orientation of the fibres to the loading direction [4], reliable criteria that can be used to predict fatigue lives under various loading conditions have not yet been established [5]. Recent advances in developing composites failure strength criteria based on whether it is the fibres, matrix or interface that are controlling [6, 7] have yet to be extended to fatigue where significant portions of the fatigue life can be taken up with breakdown of the matrix, interface and fibre. The testing described below compares fatigue behaviour under uniaxial and bi-axial bending conditions at R-ratios of R = 0.1 and R = -1.

Test Materials and Experimental Procedures

The make up and mechanical properties of the two test materials is given in Table 1. Laminates having a total of 36 plies of 781 style glass cloth were fabricated from pre-pregs made with either a 250°F curing epoxy or a 250°F curing cyanate-ester resin system. For the tests described in this paper the plies were all oriented so that the cloth fibres were in the 0° and 90° directions i.e. there were no off-axis fibres. Several different static tests were carried out in order to establish the mechanical properties of the

Table 1. Properties of Laminates used for Fatigue Testing

Material	Glass/Epoxy	Glass/Cyanate-Ester
Re-inforcement	781 style E-Glass cloth	781 style E-Glass cloth
Matrix	250°F cure Epoxy	250°F Cyanate-Ester
Number of Plies	36	36
Thickness (mm)	8.8 ± 0.3	9.4 ± 0.1
0° (or 90°) Flexural Properties, ASTM D 790, 5 tests		
Modulus (GPa)	21.7 ± 0.82	21.8 ± 0.40
Failure Stress (MPa)	429 ± 15	451 ± 16
Failure Strain (%)	2.44 ± 0.08	2.60 ± 0.17
45° Compression Properties, ASTM D 695 type fixture, 3 tests		
Modulus at 45° (GPa)	11.4 ± 0.3	13.7 ± 0.4
Stress at 2.5% Strain (MPa)	106 ± 1	127 ± 1
Interlaminar Shear Properties, ASTM D 3846, 3 tests		
Failure Stress (MPa)	56.0 ± 1.7	54.6 ± 3.6

laminates. Flexural strength and flexural modulus were obtained from four point bend tests carried out in accordance with ASTM D-790, while stress-strain curves were generated on samples cut at 45° to the fibre directions by loading in compression. Interlaminar shear strength was measured using a scaled up version of the ASTM D 3846 test method.

Figure 1 shows the four-point bending arrangement used for the R = 0.1 fatigue tests. Four point bending rather than three point bending was chosen so that a relatively large volume of material was subjected to the maximum, well defined cyclic stresses. The span, L, was 300 mm while the specimen width was 20 mm. The outer loading pins were fixed and mounted on the load frame actuator while the inner loading pins were attached through a pivot pin to the load cell. Steel cylinders were placed over the loading pins to accommodate the longitudinal displacements in the test specimens and to help reduce the contact stresses. The inner cylinders were covered with a layer of rubber to further reduce the magnitude of the contact stresses. This arrangement worked very well, for the most part, producing relatively few failures directly under the inner loading pins. Fatigue testing was carried out under load control using a constant load amplitude from the beginning to

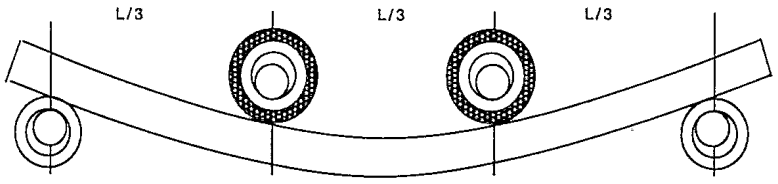

Figure 1. Loading Arrangement for R=0.1 Beam Tests.

the end of each test. An extensometer was mounted between the inner loading pins on the tensile side of the specimen at the start of each test in order to record the load - strain response over the first few cycles. The tests, which were run at frequencies of between 2 and 5 Hz, were continued until the specimens broke.

The loading arrangement for the reverse bending, R = -1, tests was similar to that used for the R = 0.1 tests except that a double set of rollers was needed. The vertical distance between the rollers was adjusted so that no pinching of the specimens took place even at maximum deflection. Test frequencies were generally half of that used for the R = 0.1 tests although the capability of the hydraulic actuator was limiting in some tests. Extensometers, this time mounted on both the tensile and compression sides of the specimen, were again used to monitor the initial load - strain response.

For the bi-axial fatigue tests a plate bending fixture was built in such a way as to incorporate many of the features of the beam bending tests. A section through the circular fixture is shown in Figure 2. The diameters of the outer support ring and inner loading ring were kept approximately the same as the distances between the outer and inner loading pins in the beam tests. Twenty four curved segments were placed around the outer ring to increase the inward displacement of the plate as the simply supported edges rotated freely under load. The inner loading ring was machined as a single piece and then cut into twelve 30° segments, each one having a depression in the centre to locate a loading pin. A layer of reinforced rubber was placed beneath the twelve loading pads in order to help ensure that there was an even pressure around the ring. Strain gages were mounted at the centre of each plate on both the top and bottom surfaces. Tests were again run with a constant load amplitude, usually at a frequency of between 1 and 2 Hz.

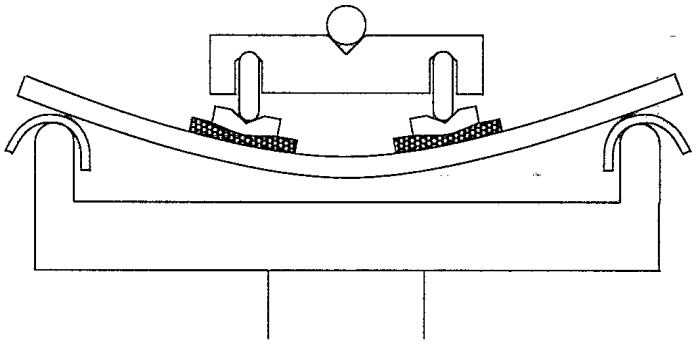

Figure 2. Loading arrangement for bi-axial fatigue tests.

Test Results

Beam Tests. The results of the R = 0.1 fatigue tests are shown in Figure 3. The fatigue lives are plotted against the tensile strain corresponding to maximum load at the start of each test since all of the failures initiated on the tensile sides of the specimens. Similar data for the R = -1 tests are plotted in Figure 4. Because of the reverse bending and the almost identical tensile and compressive moduli, both sides of the specimens experienced alternating tensile and compressive strains of the same magnitude. Consequently, there was no difference between the top and

bottom surfaces of the test specimens and no preference for initiation of failure. The data in Figures 3 and 4 shows that there was no significant difference in fatigue behaviour between the two materials.

Plate Tests. The strain gage measurements provided some insight into the nature of the loading actually present in the plate tests. The three outputs from a 0/45/90 rosette gage mounted at the centre of the tensile side of a plate are plotted against load in Figure 5 (a). The three curves fall on top of each other indicating that the bi-axial strains are essentially independent of direction. The uniformity of the strain field within the area of the inner loading ring was investigated by loading another plate in three different positions. Back to back gages were used to measure the surface strains at the three positions shown in the inset of Figure 5 (b). The good agreement between the three curves shows the uniformity of the strain field over the portion of the plate lying within the loading ring. A comparison of the magnitude of the tensile and compressive strains in Figure 5 (b) reveals that significant diaphragm stresses develop in the

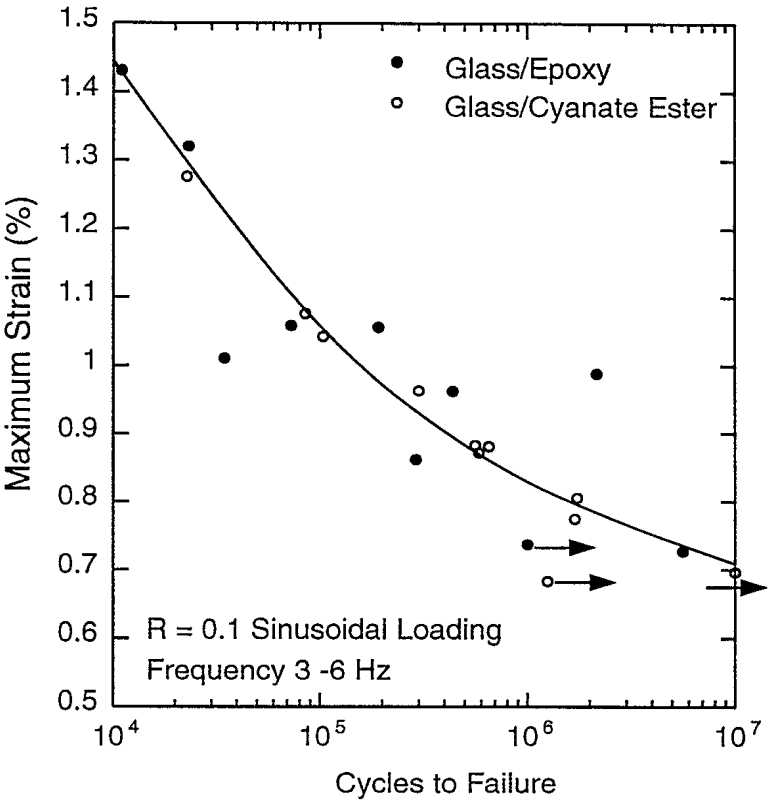

Figure 3. Strain - N curve for R=0.1 specimens.

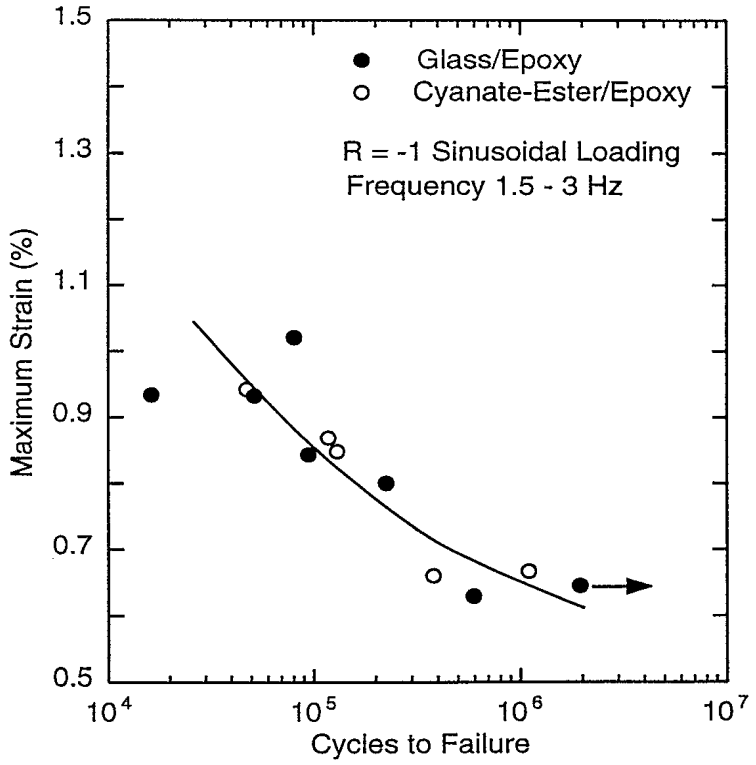

Figure 4. Strain - N curve for R=-1 specimens.

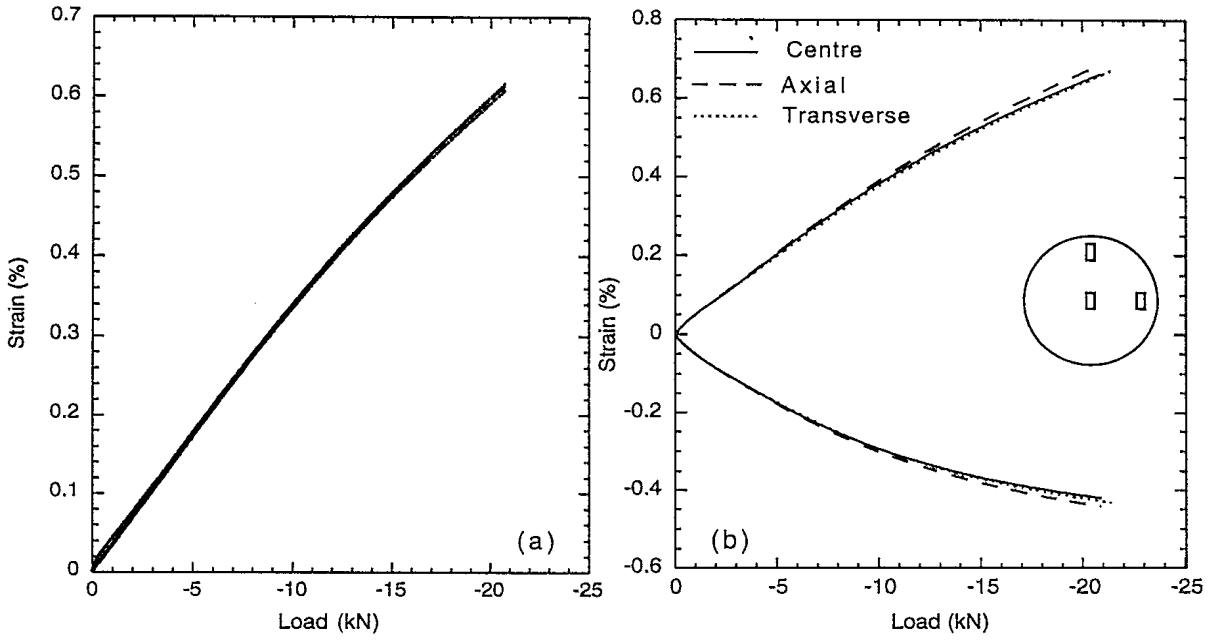

Figure 5. Load - Strain curves for bi-axially loaded panels. (a) 0, 45 and 90° strains at centre of panel, tensile side. (b) 0° strains at 3 positions, both sides.

plate as the load-strain curves become non-linear.

Some results from the plate tests are shown in Figure 6. The number of cycles to failure for six different test plates is plotted against the maximum tensile strains measured at the start of each test. All of the failures initiated on the tensile side of the plates and all were very similar in

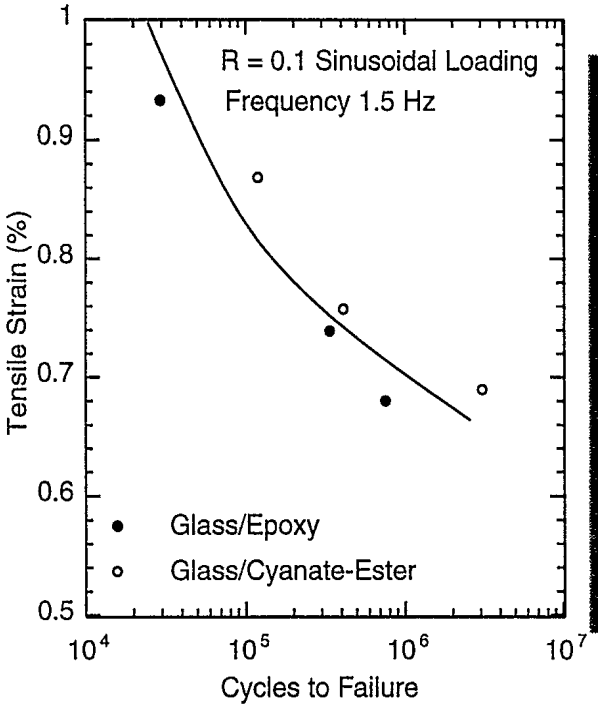

Figure 6. Bi-axial fatigue data.

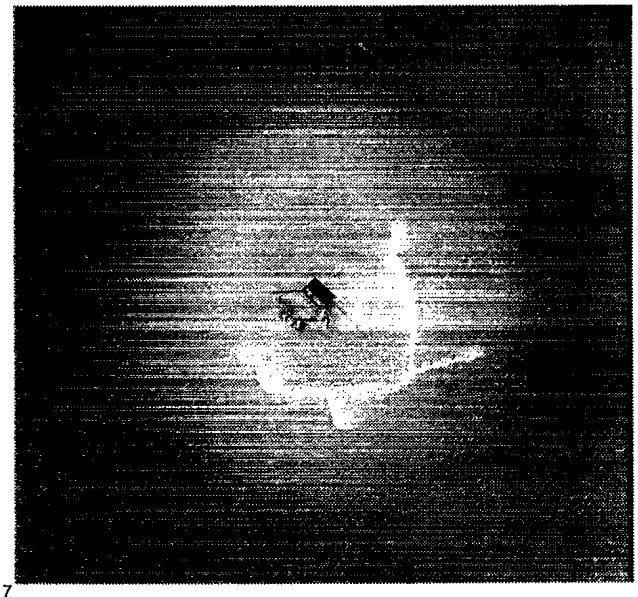

Figure 7. Failure on tensile surface of fatigue loaded glass/epoxy panel.

appearance. Figure 7 shows the final fractures on the tensile side of a glass/epoxy panel as well as a large "whitened" area in the centre of the plate.

All of the fatigue results have been summarized in Figure 8. Owing to the

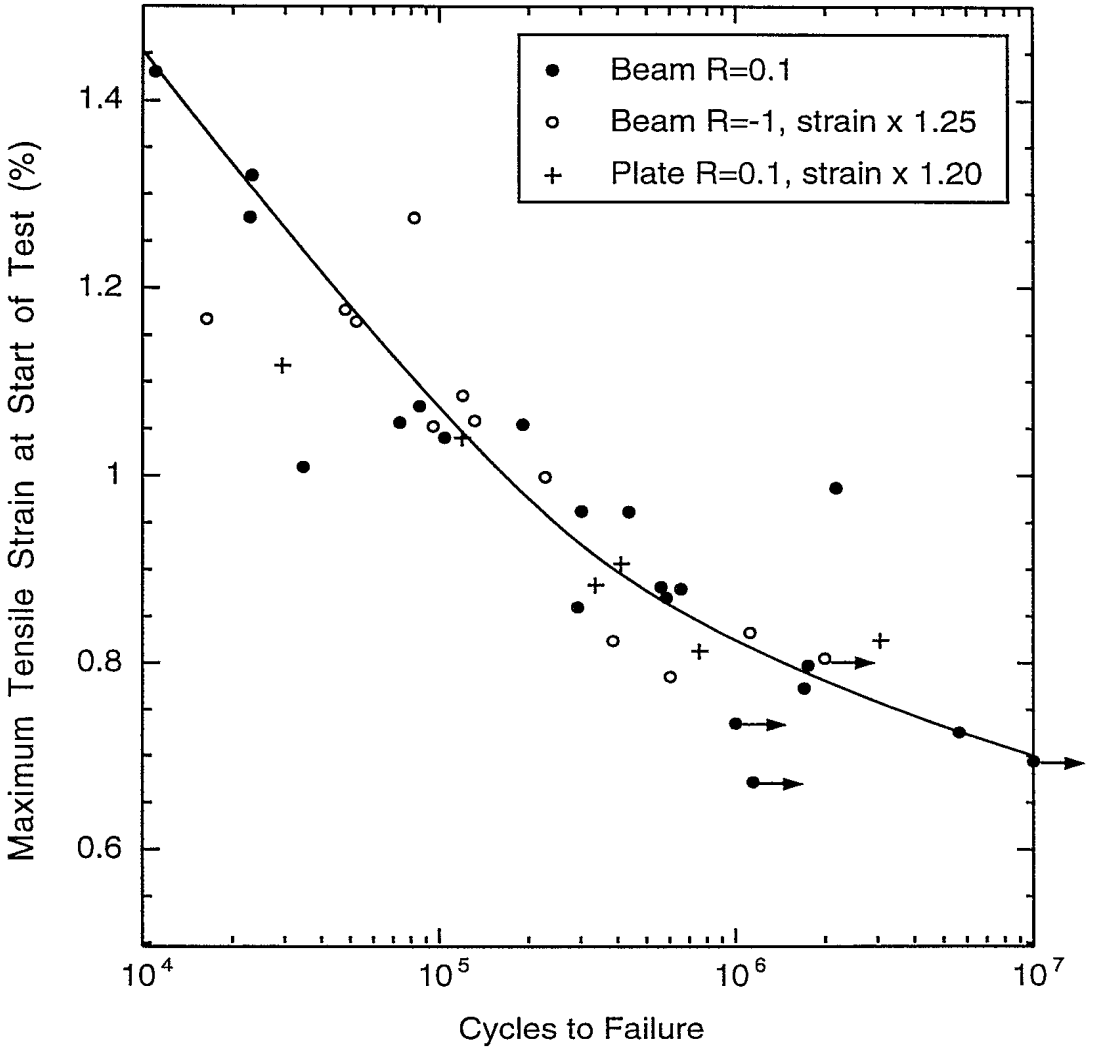

Figure 8. Summary of fatigue data from all three loading conditions.

absence of any significant difference in fatigue life between the two materials, all of the data from the same type of test have been grouped together. A best fit superposition of the strain - cycles to failure data from each of the three tests was achieved by multiplying the R = -1 strains by a factor of 1.25 and the bi-axial strains by a factor of 1.20. In terms of designing for fatigue loads a threshold strain of approximately 0.7% would suffice for uni-axial, uni-directional loads but a lower limit of between 0.55 and 0.6% strain would be required for bi-axial or reversed bending loads. No testing of these materials has yet been carried out to determine the effect of combining bi-axial loading and reversed bending.

IMPACT TESTING

Although it is well recognized that composite laminates are susceptible to damage resulting from out-of-plane impacts, there is a shortage of design approaches that can model both the structural and material responses effectively. Impact testing tends to be empirical in nature with little or no capability to predict from one set of test variables (impactor shape, mass and velocity, laminate thickness and boundary conditions) the response to a different set of test conditions [8]. As such, it is generally used to rank material systems and to indicate the likely modes of failure which can range from micro-cracking of the matrix and/or fibre/matrix interface through delamination of the plies to tensile failure of the back surface plies. As well as providing this kind of information the impact testing described here was intended to generate dynamic data that could be used to calibrate dynamic 3-D models of composite structures under impact loading conditions. Recently, progress has been made towards developing composites failure criteria that can be incorporated into analytical models of this kind [9,10].

With sonar dome applications, there are two distinct concerns related to impact damage. In addition to the cost and disruption generally associated with structural repairs there is also the degradation in performance that can result from a reduction in sound transmission or from an increase in flow generated noise. Three different elastomers were therefore evaluated in terms of their ability to protect the underlying laminate from damage caused by impact.

Experimental Procedures

Figure 9 shows the arrangement used to carry out the drop weight impact tests. The steel support ring, which was approximately 250 mm in diameter and 75 mm in height, rested on a 50 mm thick steel plate on a large concrete foundation. The circular loading tup had a slightly curved impact surface and was instrumented with 4 strain gages on the necked down portion. The tup was screwed into an aluminum crosshead which was in turn constrained to slide vertically up and down by two plated steel columns. Drop heights ranged from 0.5 to 2.5 metres and weights from 5 to 25 kg giving an energy range of between 25 and 600 J. A Nicolet storage scope was used for data acquisition, and signals were collected from the tup, from a displacement gage and from a strain gage mounted on the back surface of the test panel directly below the impact point. For the tests reported here 10 mm thick panels were fabricated from 40 plies of the same glass/epoxy pre-preg system as that used for the fatigue tests. Elastomeric coatings, as described

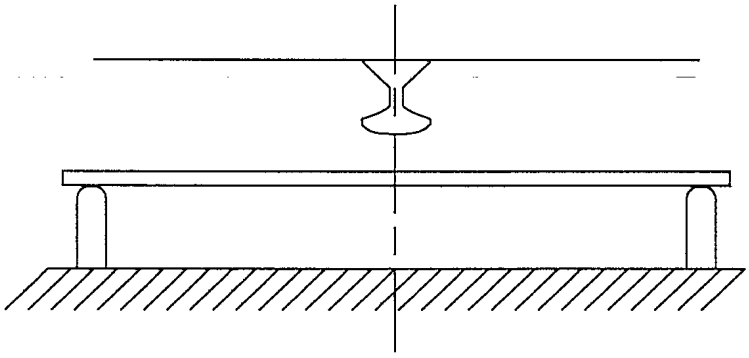

Figure 9. Arrangement used for low velocity impact tests.

in Table 2, were applied to the front surface of four of the panels. A mass of 21.3 kg and a drop height of 2.0 m was used for these tests since the resulting energy of 418 J was just sufficient to produce failure in an unprotected panel.

Table 2. Elastomeric Coatings Applied to Four Impact Panels

Elastomer	Colour	Thickness (mm)
Natural Rubber	Tan	12.7
Polyurethane (thermoset)	Black	12.7
Polyurethane (thermoset)	Black	6.4
Plasticized PVC	Blue	12.7

Test Results

In preliminary tests, in which multiple impacts at progressively higher energies were inflicted on the same panel, micro-cracking began to appear on the bottom of the panels below the impact point at energies of around 60 J. The severity and extent of the micro-cracking increased very gradually until the back-surface ply failed under tension at an energy of close to 400 J. No delamination was observed prior to failure of the back-surface ply. Figure 10 shows plots of the back surface strain versus time for the four elastomer coated glass/epoxy panels as well as for an unprotected panel.

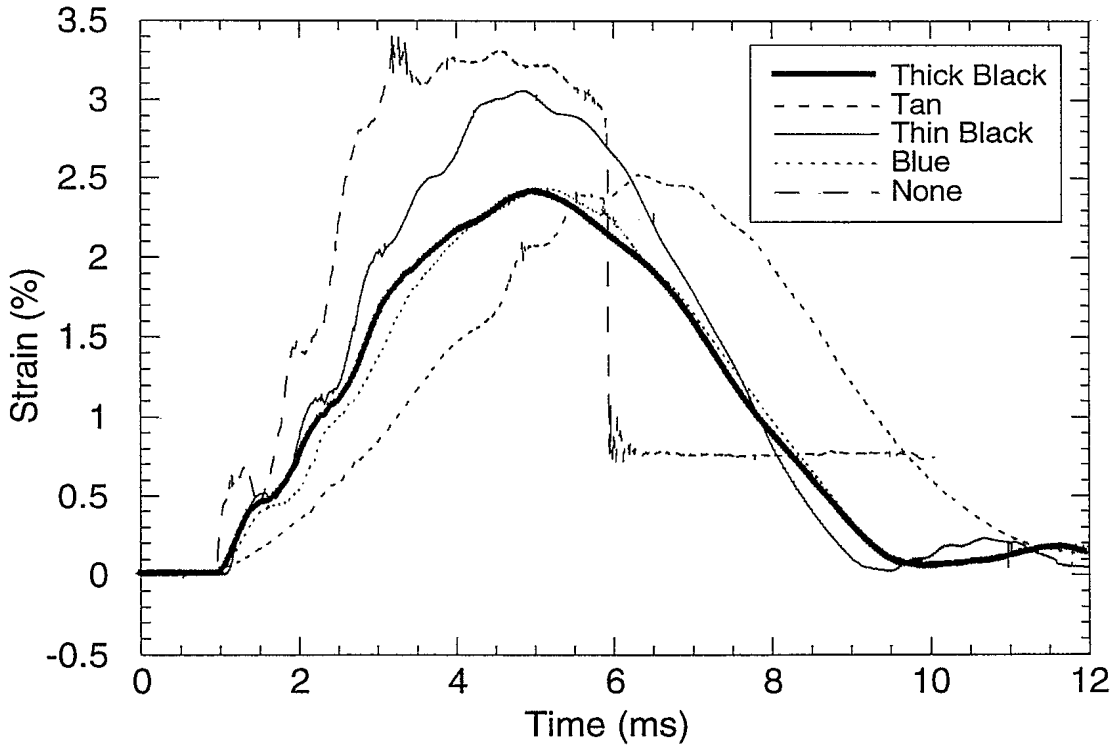

Figure 10. Effectiveness of elastomeric coatings at reducing impact induced back surface strains.

Initiation of failure in the unprotected panel can be seen as the small drop in strain from 3.3% to 3.0%. (The sharp decrease in signal at 6 ms is caused by failure of the gage). All three elastomers produced similar reductions in the magnitude of the back surface strain although the natural rubber gave the greatest reduction in loading rate because of its lower modulus. The ability of the other two elastomers to withstand repeated impacts is compared in Figure 11. While the peak strain measured on the back of the

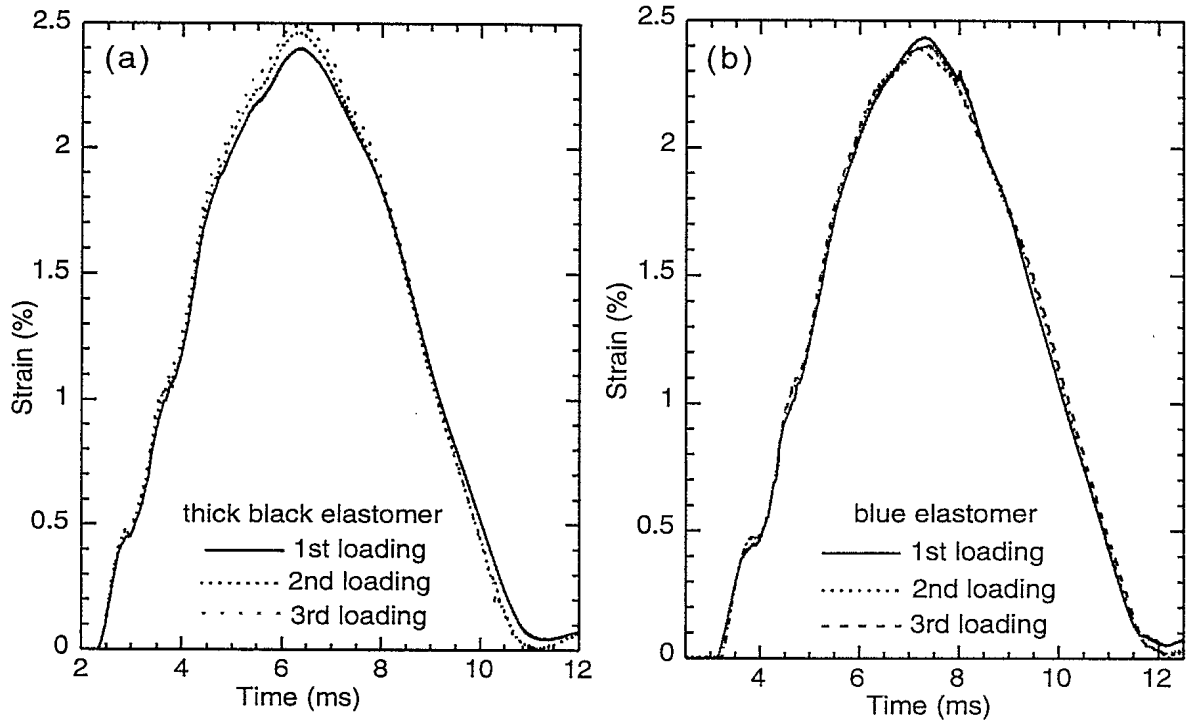

Figure 11. Comparison of back surface strains on elastomer coated panels during first, second and third impacts. (a) 12.7 mm of polyurethane. (b) 12.7 mm of PVC.

panel coated with the polyurethane increased to 2.46% (from 2.40%) on the second impact and to 2.52% on the third impact, the effectiveness of the PVC did not appear to deteriorate and no evidence of crushing or denting was apparent. The strain - time curves in Figure 11 also show the excellent reproducibility of the impact response achieved in these tests.

DAMAGE CHARACTERIZATION

Although the whitening of the laminates that occurred during fatigue and after sub-critical impacts was quite visible, no non-destructive method of quantifying the extent and nature of the micro-cracking proved satisfactory. Ultrasonic C-scans could be configured to show the presence of the micro-cracking but the changes were very subtle and only the overall size of the damage zone could be determined. While the opacity of the laminate indicated that damage was present the large number of plies again blurred any detail. Low power microscopy of the laminate surface, illuminated from above, showed individual cracks, but only within a few plies of the

surface. For example, Figure 12 shows the contrast in crack distribution between the glass/epoxy and glass/cyanate-ester panels subjected to 60 J low velocity impacts. Polished samples cut from test specimens provided the

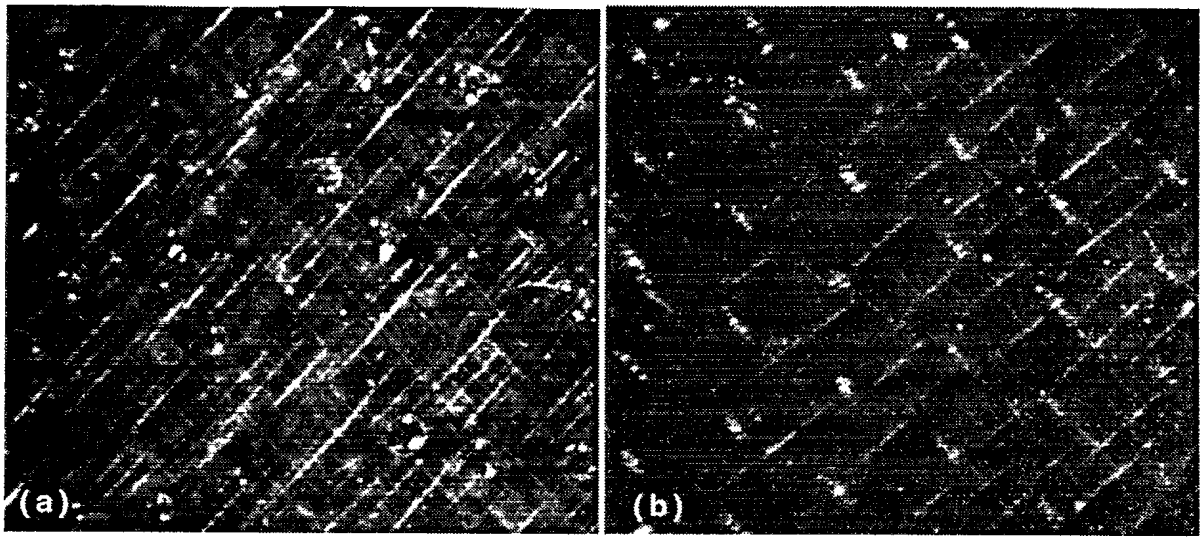

Figure 12. Top lit images of micro-cracking on tensile side of panels subjected to 60 J impacts. (a) glass/epoxy, (b) glass/cyanate-ester. Panels oriented at 45°.

most detailed information, but could not be used for monitoring damage growth. Typically, micro-cracks were found within and between the fibre tows running parallel to the fibres. For uni-axially loaded specimens cracking was limited to the 90 degree oriented tows. While micro-cracking in the glass/epoxy was found within the tows, Figure 13 (a), cracks in the cyanate-ester laminates appeared to initiate within the resin rich regions between the tows and then extend between the fibres, Figure 13 (b). Delamination type cracks, running between the tows and along the edges of the tows, were observed in the reverse loaded specimens only, Figure 13 (c), presumably driven by the compressive stresses. Figure 13 (d) shows a crack running through a 0° tow, although in general, there were very few of these cracks. This made it very difficult to ascertain to what extent their formation was influenced by the matrix cracking already present.

ON-GOING WORK

The testing described above was intended to provide baseline data and to establish a relatively inexpensive methodology for investigating long term durability. As such, it has met both these goals although work on the influences of seawater and temperature excursions, particularly freezing, are still progressing. One of the techniques that has proven of value in determining the stability of matrix materials exposed to moisture is Raman spectroscopy. For example, peaks associated with un-reacted curing agent that diminish with moisturizing time can indicate material systems that will eventually degrade because of the dissolution of water soluble components. Other on-going testing of these glass fabric composites includes fatigue testing of moisturized panels and impact testing of panels

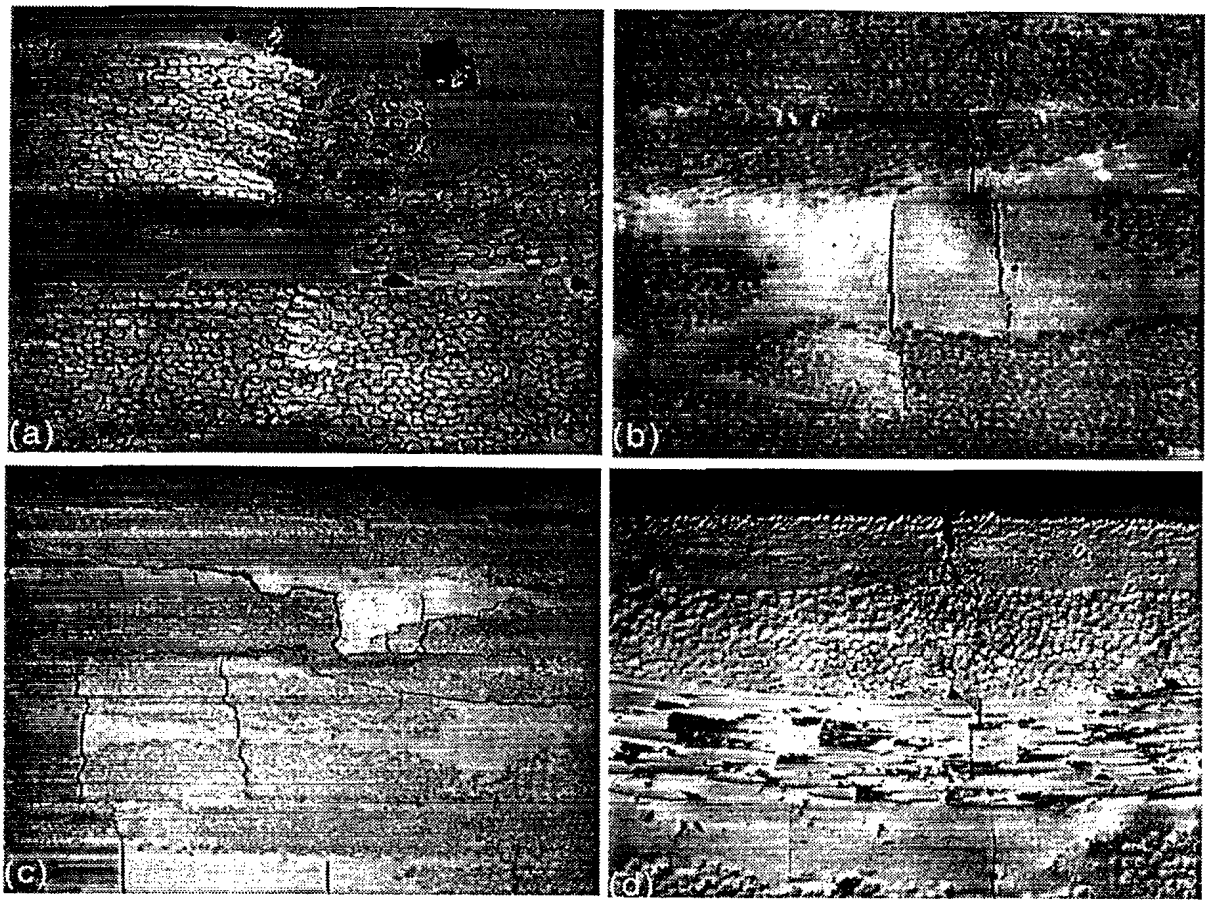

Figure 13. Polished sections taken from test specimens. (a) Glass/epoxy, bi-axial fatigue, (b) glass/cyanate-ester, bi-axial fatigue, (c) glass/cyanate-ester, R=-1, (d) glass/cyanate-ester, R = 0.1. a,b and c sectioned at 45 degrees. d sectioned parallel to loading direction.

having off-axis fibre orientations and different thicknesses. A longer term goal is to generate similar data on a number of composite material systems fabricated by resin transfer moulding so that some consideration can be given to optimizing long term durability as part of the design process.

ACKNOWLEDGEMENTS

The mechanical testing expertise of Dan Liesch, the metallographic skills of Paul Martin and the chemistry support provided by Bob Rowland are all gratefully acknowledged.

REFERENCES

[1] R.A. Shenoi and J.F. Wellicome, Ed., "Composite Materials in Maritime Structures", Volumes 1 and 2, Cambridge University Press, 1993.

[2] F. Pomies, L.A. Carlsson, D. Choqueuse and P. Davies, "Degradation of Composite Materials in a Marine Environment: New Materials and Test Methods", Nautical Construction with Composite Materials, pp. 375-385, IFREMER, 1992.

[3] R. Talreja, "Fatigue of Composite Materials", Technomic Publishing Co., 1987.
[4] M.J. Salkind, "Fatigue of Composites", STP 497, pp. 143-169, ASTM, 1972.
[5] E. Greene, "Design Guide for Marine Applications of Composites", SSC-403, Ship Structures Committee, c/o US Coast Guard, 1997.
[6] L.J. Hart-Smith, "A Scientific Approach to Composite Laminate Strength Prediction", STP-1120, pp. 142-169, ASTM, 1992.
[7] L.J. Hart-Smith, "The First Fair Dinkum Macro-Level Fibrous Composite Failure Criteria", Proceedings of ICCM-11, Vol. 1, pp. 52-87, 1997.
[8] J.S. Peraro, "Prediction of End-Use Impact Resistance of Composites", STP 936, pp. 187-216, ASTM, 1987.
[9] K. Williams and R.Vaziri, "Finite Element Analysis of the Impact Response of CFRP Composite Plates", Proceedings of ICCM-10. pp. 647-654, 1995.
[10] J. van Hoof, M. Worswick, P.V. Stranznicky, M. Bolduc and S. Tylko, "Finite Element Response of Composite Helmet Materials", Proceedings of ICCM-11, Vol 2, pp. 532-539, 1997.

#S07459